



# Structural, optical, and electrical properties of ferroelectric copolymer of vinylidene fluoride doped with Rhodamine 6G dye

Cite as: J. Appl. Phys. 125, 044103 (2019); <https://doi.org/10.1063/1.5067272>

Submitted: 16 October 2018 . Accepted: 05 January 2019 . Published Online: 31 January 2019

V. V. Kochervinskii, M. A. Gradova, O. V. Gradov, D. A. Kiselev, T. S. Ilina , A. V. Kalabukhova, N. V. Kozlova, N. A. Shmakova, and S. A. Bedin 



View Online



Export Citation



CrossMark

## Ultra High Performance SDD Detectors



See all our XRF Solutions

# Structural, optical, and electrical properties of ferroelectric copolymer of vinylidene fluoride doped with Rhodamine 6G dye

Cite as: J. Appl. Phys. **125**, 044103 (2019); doi: [10.1063/1.5067272](https://doi.org/10.1063/1.5067272)

Submitted: 16 October 2018 · Accepted: 5 January 2019 ·

Published Online: 31 January 2019





View Online



Export Citation



CrossMark

V. V. Kochervinskii,<sup>1</sup> M. A. Gradova,<sup>2</sup> O. V. Gradov,<sup>2,3</sup> D. A. Kiselev,<sup>4</sup> T. S. Ilina,<sup>4</sup>  A. V. Kalabukhova,<sup>1</sup> N. V. Kozlova,<sup>1</sup> N. A. Shmakova,<sup>1,5</sup> and S. A. Bedin<sup>6</sup> 

## AFFILIATIONS

<sup>1</sup>Karpov Institute of Physical Chemistry, Moscow, Vorontsovo Pole, Russia

<sup>2</sup>Semenov Institute of Chemical Physics, Russian Academy of Sciences, Moscow, Russia

<sup>3</sup>Tal'rose Institute for Energy Problems of Chemical Physics, Russian Academy of Sciences, Moscow, Russia

<sup>4</sup>National University of Science and Technology "MISIS," Moscow, Russia

<sup>5</sup>Enikolopov Institute of Synthetic Polymeric Materials, Russian Academy of Sciences, Moscow, Russia

<sup>6</sup>Moscow Pedagogical State University, Moscow, Russia

## ABSTRACT

An effect of Rhodamine 6G dye introduced into vinylidene fluoride and tetrafluoroethylene copolymer on a number of its structural and electrical characteristics has been detected. It was shown that at film crystallization, the inserted dopant shifts the equilibrium distribution of isomers to the side of increasing concentrations of chains with the conformation of a planar zigzag. The dye introduced strongly increases ac conductivity, especially at high electric fields. The investigation of high voltage polarization under bipolar external field conditions shows slow switching of gigantic current which is observed at fields lower than coercive ones. The estimation of the charge density indicates the non-ferroelectric nature of the phenomenon observed. The analysis of the data shows that in the system, Maxwell–Wagner relaxation processes take place, which lead to the space charge formation in the polymer matrix. It is established that current switching observed must be attributed to the relaxation of the space charge field.

Published under license by AIP Publishing. <https://doi.org/10.1063/1.5067272>

## INTRODUCTION

Ferroelectric polymers represent a relatively new class of materials. Among them, polymers on the base of polyvinylidene fluoride (PVDF) are the most widespread ones. Just like in inorganic ferroelectrics (crystals and ceramics of many kinds), in these polymers, it is possible to initiate the appearance of piezo- and pyro-electricity after polarization. Values of the majority of piezo-constants in inorganic materials turn out to be an order of magnitude higher than those in polymer ferroelectrics. Nevertheless, because of the chain nature of macromolecules, the latter have a number of specific properties which make them interesting for practical usage. The low mechanical quality factor makes it possible to use such materials as sensors with a wide dynamic diapason.<sup>1–3</sup> High shock viscosity of flexible chain crystalline polymers is another valuable property for their practical realization as pressure

sensors. This makes it possible to produce shock wave sensors on the base of ferroelectric polymers.<sup>4</sup> Crystalline polymers under consideration also contain an amorphous phase, which may reach the value of 0.5 and more. At room temperature, such a phase is in the liquid-like state. That is why such polymers demonstrate gigantic electrostriction.<sup>5</sup> Because of their high electric breakdown fields, it is possible to recommend the creation of capacity accumulators of energy on their basis.<sup>6</sup>

Doping of polymer materials is one of the methods used for modifying their properties. Since polymers studied are soluble in a number of organic solvents, it is possible to introduce molecules of dyes into them from their common solvent. It was shown earlier that spectra characteristics of Rhodamine 6G (R6G) luminescent molecules introduced into the copolymer of vinylidene fluoride (VDF) with trifluoroethylene (TFE)

turn out to be sensitive to the ferroelectric–paraelectric phase transition.<sup>7</sup> One of the applications of dyed ferroelectric polymers is associated with the possibility to investigate the phenomenon of electrochromism. A practical investigation of devices based on the application of such an effect is described in Ref. 8, where the change of the dye absorption spectrum under the influence of the electric field is demonstrated. Besides, as shown from our early works, in the structure of domains in the considered polymers, there are regions of the amorphous phase.<sup>9,10</sup> Since the introduced dye is localized in the range of the increased free volume (that is in the amorphous phase), it may be expected to affect the switching characteristics of spontaneous ferroelectric polymer polarization. In this work, the statistical copolymer of VDF with TFE has been used, the mole fraction of the last comonomer being 6%. In a previous work, we used R6G with the same copolymer, but the content of TFE was 29 mol. %.<sup>11</sup> So, in this work, the polymer matrix has a higher concentration of polar groups responsible for the formation of ferroelectricity.<sup>1,2,12</sup> It has been shown that the dye molecules introduced, which are crystallization centers, mostly promote the formation of crystals with the conformation of a planar zigzag. Besides, the intensive process of current switching, which we attribute to the switching of the space charge field formed by the dye molecules, has been registered.

## EXPERIMENTAL AND MATERIALS

The 94:6 statistical copolymer was the object of our study. According to the data of a high-resolution nuclear magnetic resonance (NMR) study, copolymer chains contain 4.5 mol. % defects “head to head (tail to tail).”<sup>13</sup>

Absorption electron spectra have been registered with the use of a HACH DR-4000 V (Hach-Lange, USA) spectrophotometer at room temperature with wavelengths in the range of 320–900 nm with 1 nm steps. The absorption spectra of dye solutions in acetone (Ac) were carried out in a quartz cuvette with 10 mm length optically. Optical microphotographs of surfaces of doped films were obtained using a BS-702 B binocular microscope equipped with a digital USB camera.

Infrared spectra were obtained on a Bruker Equinox 55s (with Fourier transform) spectrometer. Shooting was performed in transmission and attenuated total reflection (ATR, ZnSe crystal) regimes; the latter was used to probe the 0.5–2  $\mu\text{m}$  thick surface layer of the polymer. Dielectric properties were investigated by means of a Novocontrol Concept 40 broadband dielectric spectrometer in isothermal regime in the frequency range  $10^{-2}$  to  $10^7$  Hz at 20 °C. Prior to dielectric measurements, 50-nm-thick gold electrodes were deposited on films via thermal vacuum evaporation. The measurement of high-voltage polarization and conductivity was carried out on the modified setup combined according to the Sawyer–Tower scheme provided that  $C_s \ll C_0$  ( $C_s$  and  $C_0$  were capacities of the sample and the reference capacitor, respectively).

Kelvin probe force microscopy (KPFM), piezoresponse force microscopy (PFM), and switching spectroscopy were

carried out with an Asylum Research MFP-3D atomic force microscope, using the CSG30/Pt conductive probe with the spring constant of 0.6 N/m. For KPFM measurements, the probe scanned the surface topography using a tapping mode. 1 V AC voltage was applied to the probe near its frequency ( $\sim 48$  kHz) to measure the sample surface potential distribution through a DC voltage feedback loop. All KPFM mappings were performed at room temperature with the lift height of 30 nm, and 3 V DC voltage was applied to the probe. The drive amplitude for PFM scanning was 1 V. All the poling processes were conducted in contact-mode by applying DC voltages ( $\pm 50$  V) to the conductive tip.

## RESULTS

First, it should be proper to consider data for the original dye solution, which will be added to the polymer solution. As seen from Fig. 1(a), the absorption spectra change notably

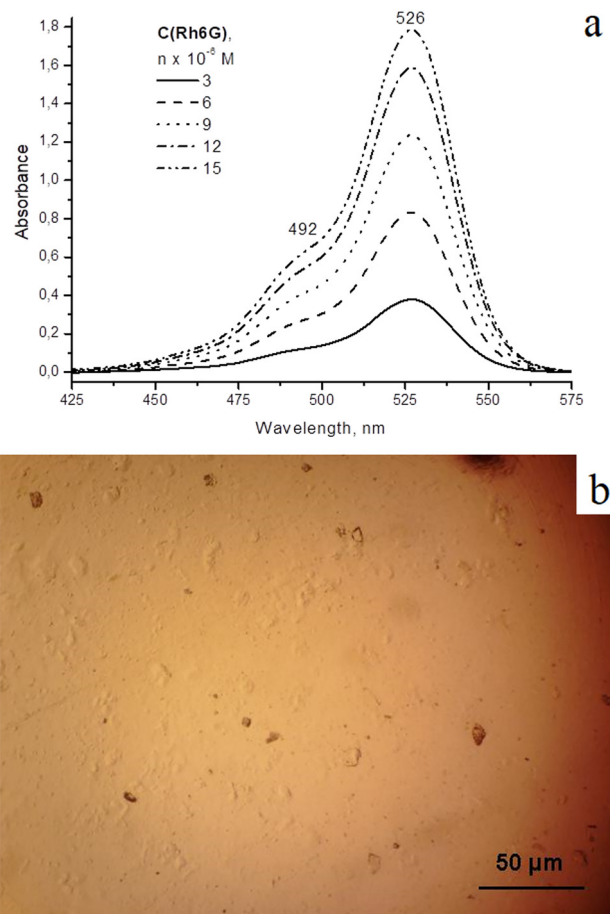


**FIG. 1.** (a) Electron absorption spectra for a series of solutions with different R6G concentrations in acetone. (b) Optical microphotography of the copolymer doped film with R6G concentration 0.2%.

with an increase in the dye concentration. Analysis shows that at the chosen concentrations, the dye exists at any rate in two forms: dimer (D) and monomer (M). Absorption bands 492 and 526 nm relate to the first and second forms, respectively.<sup>14</sup> As it can be seen from Table I, the results show that an increase in the dye concentration leads to an increase in its dimer form content. It is seen that at the dye concentration higher than  $10^{-5}$  mol/l, signs of aggregation are observed. Deflections from linear dependence of Burger–Lambert–Beer law and increasing ratios of optical densities of absorption bands of dimer ( $\lambda_D = 492$  nm) and monomer ( $\lambda_D = 526$  nm) forms of the R6G dye in absorption electron spectra indicate it. The formation of higher orders than dimers should not be ruled out.

Data on dye solutions obtained may also be used at interpretations of the structure formation in ferroelectric films also. As it has been noted above, films were formed by crystallization of the doping polymer from a common solvent. At slow solvent removal, it is equal to an increase in dye concentration in the rest of the solution. It will promote the aggregation of R6G molecules to the level of dimers and more complex formations. At considerable lowering of the solvent content, interchain interactions of the copolymer macromolecules will become stronger, which will result in their crystallization. So, dye molecules will be displaced into the amorphous phase, which has an increased free volume. Due to this process, local R6G concentration in the amorphous phase must rise, which will intensify dye molecules' aggregation. Optical microscopy data on the doped crystallized film may be used to check such hypothesis. On the microphotograph [Fig. 1(b)], heterogeneous inclusions several microns in size are seen in the film volume. Local absorption spectra of the region of their localization show that they have been formed by R6G crystals.

Indication of the dye aggregation process in films is also obtained by the piezoforce microscopy method in the variant of Kelvin-mode. For Figs. 2(a) and 2(b), surface potential distribution patterns for initial and doped samples are shown. Since the dye used is poorly compatible with the copolymer, during crystallization, it can be displaced into the surface. Therefore, we associate light areas observed in the doped copolymer [Fig. 2(b)] with the presence of dye molecules. As shown in figure, linear dimensions of the marked areas can be of microns and above. Thus, according to this method, we also see indications of dye molecules aggregation with the formation of larger supramolecular associates.

**TABLE I.** Relations for bands height of monomer (M) and aggregated (D) forms for R6G solutions in acetone with various molar concentrations of the dye.

C, mcM	$A_D$ , 492 nm	$A_M$ , 526 nm	$A_D/A_M$
3	0.116	0.379	0.306
6	0.257	0.834	0.307
9	0.389	1.236	0.314
12	0.511	1.587	0.322
15	0.592	1.782	0.332

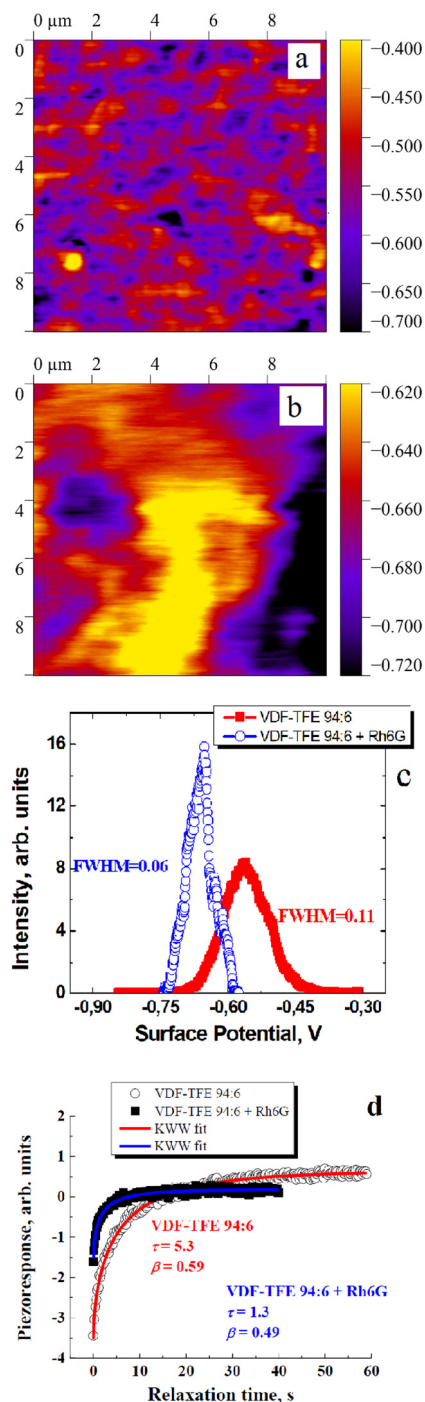


**FIG. 2.** Surface potential images of pure VDF-TFE 94:6 (a) and VDF-TFE 94:6 + Rh6G (b), the histogram distribution of surface potential for investigate copolymer samples (c), relaxation dependences of the remnant piezoelectric response signals for both samples after local poling at 50 V for 10 s (symbols) and fitting by Kohlrausch–Williams–Watts function (solid lines) (d). The inset in (c) and (d) presents fitting parameters to investigate the polymer samples.

Since this dye has an ionic nature, it can influence the copolymer crystallization process during the film formation. In particular, dye ions may be crystallization centers, and in the presence of polymorphism in the polymers studied,<sup>1,2,15</sup> they may affect the formation of one or another crystallographic modification. There are enough evidence of the correctness of such a hypothesis in the literature. There are several works<sup>16–18</sup> where it is shown that the introduction of dopants, containing ions, results in enriching the forming polymer with chains in the conformation of a planar zigzag. In this connection, we checked for such a possibility by doping the polymer studied by R6G molecules. In Fig. 3, IR spectra for various spectral intervals are shown. Figure 3(a) shows the initial (non-doped) film of the copolymer crystallizes as a mixture of  $\gamma$ - and  $\beta$ -phases. It can be judged by the presence of absorption bands 1235 and 1275  $\text{cm}^{-1}$ , where the first is sensitive to  $\gamma$ -phase  $T_3GT_3G^{-1}$  conformation and the second reflects the presence of long sequences with the conformation of a planar zigzag, characteristic of the polar  $\beta$  phase.<sup>1,2,15</sup> It is seen from the picture that at crystallization of the copolymer with this dye, intensity redistribution of bands 1235 and 1275  $\text{cm}^{-1}$  takes place. It means that the structure formation in the presence of R6G molecules is accompanied by a partial polymorph  $\gamma \rightarrow \beta$  transition that agrees qualitatively with conclusions made by authors of Refs. 16–18. The dye introduced also affects crystallization and additional structuring of the film. Demonstration of these phenomena can be seen in Fig. 3(c), where symmetrical and asymmetrical absorption bands of valent vibrations of methylene groups are presented. For the non-doped copolymer, two absorption bands are present. With regard to those for polyethylene, these bands are substantially shifted to the high frequency region because of the presence of F atoms with strong electron-acceptor properties of the chain.<sup>1,2</sup> It follows from the same figure that, if the dye is introduced, along with main bands noted, additional duplet bands at 2853 and 2926  $\text{cm}^{-1}$  observed for polyethylene appear. We studied this effect in more detail for the case of the VDF–TrFE (trifluoroethylene) copolymer.<sup>19</sup> It was shown that similar defects of chain structure may aggregate during polymerization with the formation of clusters, where  $\text{CH}_2$  groups will be isolated from  $\text{CF}_2$  groups. Usually, it is the most noticeable one for the film surface,<sup>19</sup> but in the case of our copolymer crystallization in the presence of R6G, this additional structuring is noted over the whole volume [in Fig. 3(c), transmission spectra are presented]. In Fig. 3(b), the spectra range, where the copolymer itself practically does not absorb, is shown (curve 1). However, for the doped film, a number of absorption bands are noted. Their frequency positions turn to coincide with those for the copolymer which contains less VDF.<sup>11</sup> In our opinion, such bands reflect the interactions in aggregated R6G crystals and do not depend much on a surrounding matrix.

Another task of our work was to check the following hypothesis. It is expected that dye molecules in the solvent as well as in the amorphous phase of the copolymer are in the partially dissociated state. The presence of additional current carriers in the doped film can be seen in Fig. 4. In the doped

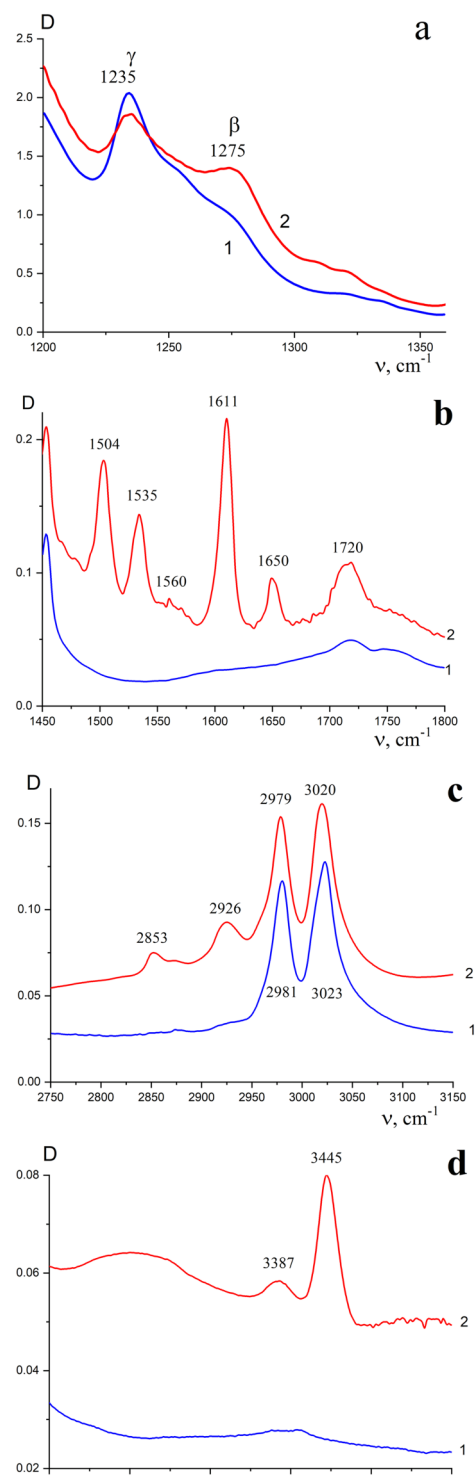


**FIG. 3.** Comparison of vibration spectra for original (1) and doped (2) copolymer films for different spectral intervals: (a) 1200–1400, (b) 1450–1800, (c) 2750–3150, (d) 3100–3600  $\text{cm}^{-1}$ .

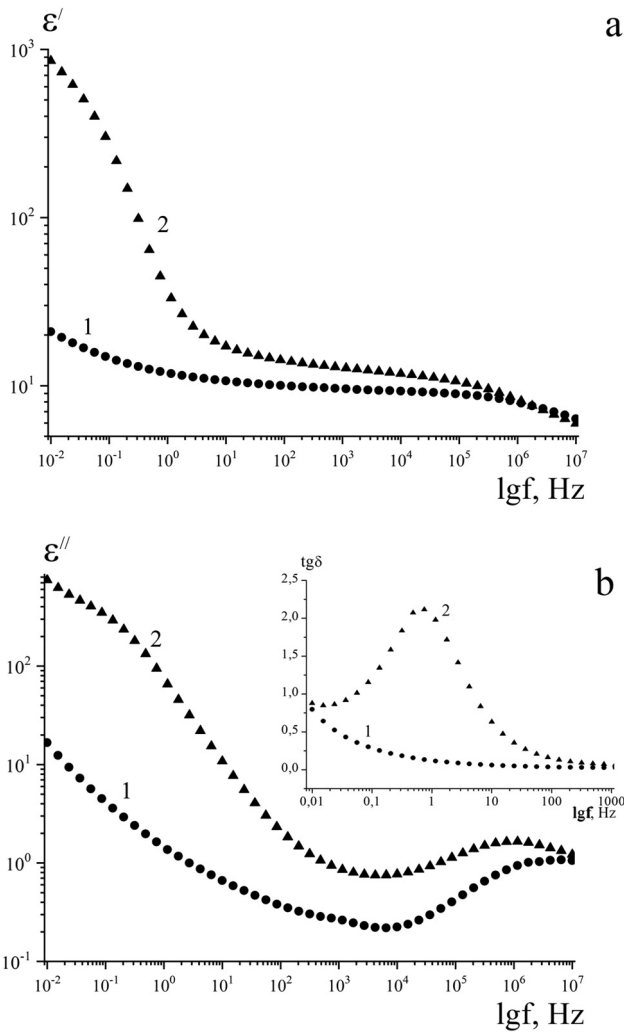


**FIG. 4.** Frequency dependencies of real (a) and imaginary (b) components of dielectric permittivity for the original (1) and doped (2) films. Inset: frequency dependencies of tangent of dielectric loss angle.

film, gigantic low-frequency dispersion [Fig. 4(a)] and weakly expressed maximum on the frequency dependence of the loss factor [Fig. 4(b)] are observed. It is seen from the inset of the last figure that the tangent of dielectric losses  $\text{tg}\delta$  has a clearly expressed maximum. Its value as well as gigantic low-frequency dispersion [Fig. 4(a)] indicates that the relaxation process observed cannot be attributed to the reaction on the field of bond charges of polymer chains. As shown in Fig. 4(b), such a process is characterized by the maximum  $\epsilon''$  in the frequency region close to 1 MHz. These data are obtained at the amplitude of an external voltage equal to 1 V. As the data from Fig. 5 show, when increasing the external source voltage, the difference in high voltage conductivity of the original and doped samples turns out to be considerably

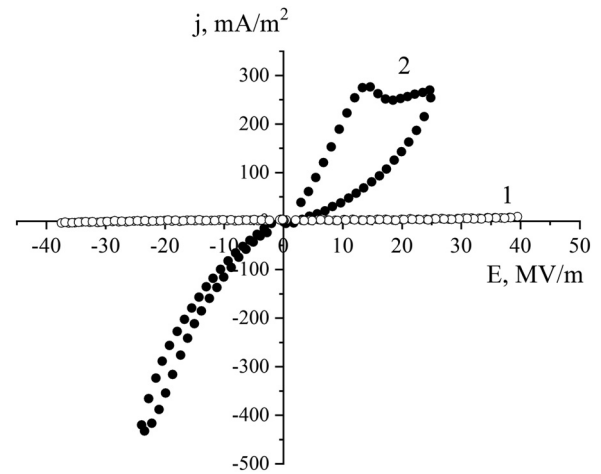


**FIG. 5.** Volt-Ampere dependencies at supplying triangle-like voltage with frequency 25 mHz to the original (1) and doped (2) copolymer films.

higher. In addition, at such high fields, current-voltage characteristics are asymmetric.

## DISCUSSION

The nature of additional current carriers in doped films must be associated with the presence of dye molecules or their aggregates in the matrix. It has been noted above that the dynamics of chains in the amorphous phase (where R6G molecules localize) at room temperature has a liquid-like nature, which is why the dye molecules will be partially dissociated just like in a solvent. Apparently, ions will be additional carriers. It can be seen from Fig. 5 that the current of a doped film will be several orders of magnitude higher than that of a non-doped one. It follows from general correlations that the current value  $j$  measured by supplying a sample with dielectric permittivity  $\epsilon$  of field  $E$  may be written as follows:

$$j(t) = j_c(x, t) + j_p(x, t) + \epsilon\epsilon_0 \frac{\partial}{\partial t} E(x, t). \quad (1)$$

The first item characterizes the conductivity current, the second one is the polarization current, and the third is the displacement current. For fields lower than coercive ones, it is possible to neglect the polarization current. At low frequencies of the field, the conductivity current will mainly contribute to the measured current

$$j_c = en\mu(x, t)E(x, t) - eD \frac{\partial}{\partial x} n(x, t). \quad (2)$$

In this equation, the second item characterizes diffusion contribution. If it is ignored, a higher current in the doped film as well as concentration will be determined by field  $E$ . It seems

that in our case, the mechanism of such influence is described by the Pool-Frenkel equation<sup>20</sup>

$$j_{PF} = n_T \mu q E \exp \left[ -\frac{E_{T_0} - \beta_{PF}(E)^{\frac{1}{2}}}{kT} \right]. \quad (3)$$

The role of the field is only to diminish the potential barrier at carriers' drift. As shown in Fig. 6, for the dye R6G, additional ions in the copolymer differ substantially in size and, consequently, in mobility  $\mu$ , which is why the response of the doped films to low-frequency electrical field must depend on the sign of the potential supplied, as is seen in Fig. 5. When supplying triangle-like voltage to the sample, at the positive direction of the field, current switching is seen. This means that anions contribute to the signal. In accordance with Fig. 6, switching current should be associated with the reaction in the field of the counterions  $\text{Cl}^-$  of the dissociated molecule R6G.

Such details could be seen in Fig. 7, where 10 s long bipolar rectangular voltage pulses were supplied to the doped film. At low voltages of an external source [Figs. 7(a) and 7(b)], it can be seen that the current for the whole half-period reveals monotonous decrease. According to Eq. (2), at constant amplitude of the external voltage, it is reasonable to attribute this to a decrease in the concentration of  $\text{Cl}^-$  ions. Since the matrix is dielectric, these ions will be trapped. Since the polymer relates to the class of ferroelectrics and crystallizes as a mixture of polar crystals of  $\beta^-$  and  $\gamma^-$  phases,<sup>1,2,15</sup> in this case, the polar planes of such crystals will be the deepest traps. The scheme of such a trapping is shown in Fig. 8. In light of such conception, a decrease in the current during the positive half-period of the field applied [Figs. 7(a) and 7(b)] may characterize kinetics of ion  $\text{Cl}^-$  trapping process by polar planes of  $\beta^-$  and  $\gamma^-$  phases. According to Fig. 6, a xantene group, where the positive charge of the quaternary nitrogen atom is delocalized, is another ionic fragment of the dissociated R6G molecule. It may be conceived that this group can interact with fragments of amorphous phase chains. Earlier, such an effect was shown with the use of another VDF

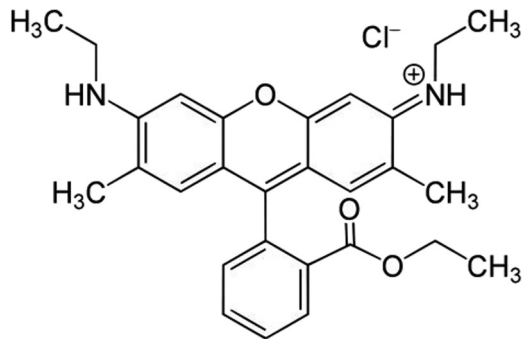


FIG. 6. Structural formula of the Rhodamine 6G molecule.

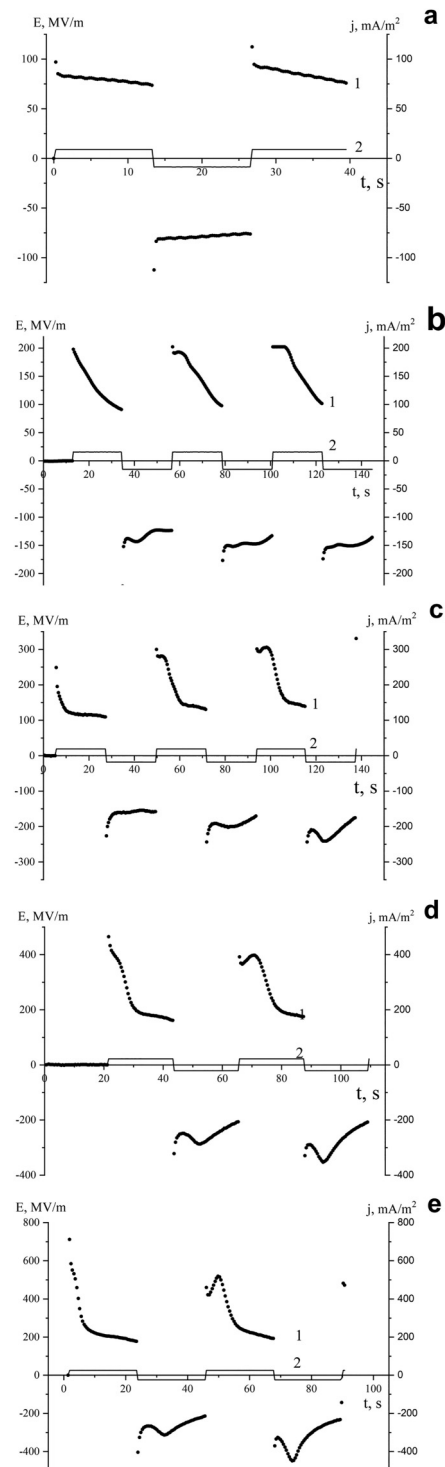
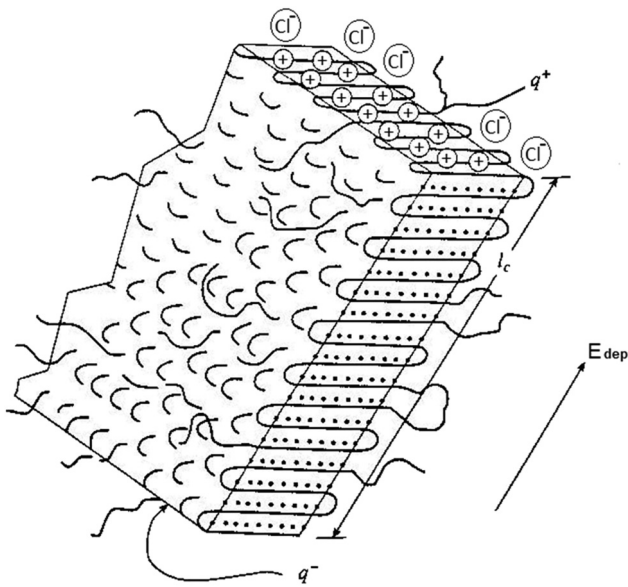


FIG. 7. Time dependencies of current through the doped film (1) when supplied with bipolar rectangular pulses of electric field (2) of different voltages: (a) 9, (b) 14, (c) 18, (d) 22, and (e) 25 MV/m.



**FIG. 8.** Scheme of trapping of ions  $\text{Cl}^-$  by polar planes of lamellar crystals of  $\beta^-$  and  $\gamma^-$  phases.

copolymer doped with the same dye.<sup>11</sup> To check such a hypothesis for the copolymer studied in this work, the IR spectroscopy method has been applied. In Fig. 3(d), the spectrum region, containing no non-doped film bands, was shown. But they appeared after R6G introduction. Just like in our previous work,<sup>11</sup> the doublet  $3445, 3387 \text{ cm}^{-1}$ , which characterizes valent vibrations, respectively, of free and bond N-H groups, is observed. We suppose that the linked state of the N-H group on condition of R6G localization in the amorphous phase may be realized by the formation of hydrogen bonds of the N-H...F-C type. R6G dimerization in the film as well as aggregation of the dye to the level of microcrystals formation [Figs. 1(b) and 2(b)] contains the possibility of the formation of three-dimensional net of labile bonds. The copolymer structuring noted above, which has been observed because of the “anomaly” in the region of valent vibrations of methylene groups [Fig. 3(c)], may reflect such processes. Conductivity during the negative half-period of the external field may be accompanied by breaking hydrogen bonds and shift equilibrium to the free N-H group formation side.

As it is shown below, the increased ionic conductivity in the doped film leads to a change in the nanoscale distribution of surface potential. To gain better statistics, we performed a histogram analysis of surface potential for pure copolymer and doped films [Fig. 2(c)]. As it can be seen, the full-width-at-half-maximum (FWHM) value of the pure (undoped) film is two times as high as that of the doped one. Besides, the surface potential signal distribution shows that the pure copolymer on average exhibits a potential signal is less than a doped copolymer film, i.e.,  $-0.56 \text{ V}$  for pure copolymer and

$-0.65 \text{ V}$  for doped film. We believe that both facts have the same cause. As it has been shown above, film crystallization in the presence of dye is accompanied by partial polymorph transformation  $\gamma \rightarrow \beta$  [Fig. 3(a)]. It is known that polar planes of  $\beta$ -phase crystals are characterized by the higher value of the surface charge density.<sup>1,2,15</sup> If these planes appear on the surface, in the case of the doped film, its surface potential must increase. Only this is observed in the experiments [Fig. 2(c)]. The film surface potential forms due to the presence of polar  $\beta$ - and  $\gamma$ -phases. It means that the FWHM value, which is shown in Fig. 2(c), will depend on the ratios of these crystals. If at dye introduction the share of the  $\beta$ -phase increases at the expense of the  $\gamma$ -phase, it must result in the narrowing of the distribution of the surface potential. This is also shown in Fig. 2(c).

It is seen from Figs. 7(c)–7(e) that the rise in amplitude creates the tendency to reveal the switched current maximum as it is usually observed in the case of ferroelectrics. According to such a mechanism, the field must be higher than the coercive one. For our polymers, it is equal to  $50 \text{ MV/m}$ . As shown in Fig. 7, the field of the external source  $E_{\text{ext}}$  is several times lower than this value. It may be seen from the same figure that switching time is about tens of seconds that is not characteristic of classical switching of ferroelectrics spontaneous polarization. Full surface density of the switched charge  $\sigma$  has been estimated as follows:

$$\sigma = \int_{t_1}^{t_2} j(t) dt, \quad (4)$$

where  $j(t)$  is the density of switched current during the period of time  $\Delta t = t_2 - t_1$ . Estimation shows that the charge density is about  $4 \text{ C/m}^2$ . It turns out to be more than an order of magnitude higher than that at polar  $\beta$ -modification ( $0.13 \text{ C/m}^2$ ).<sup>1,2</sup> All this means that the presented data do not characterize ferroelectric switching itself, but reflect some other process. Taking into account that the copolymer is heterogenic (at any rate two-phase system), where phases differ in conductivity and dielectric permittivity, it may be a Maxwell–Wagner (MW) polarization.

The accumulation of  $\text{Cl}^-$  ions on polar planes of crystals noted above will be one of the stages to form the field of the space charge  $E_{\text{sc}}$  which may be presented for the one-dimensional case as follows:

$$E_{\text{sc}}(x, t) = \int_0^d \frac{\rho(x, t)}{\epsilon_0 \epsilon} dx \int_0^\infty dt, \quad 0 \leq x \leq d, \quad (5)$$

where  $\rho(x, t)$  is the volume density of the space charge and  $\epsilon$  is the dielectric permittivity of the sample with thickness  $d$ . Frequency dependency component  $\epsilon^*$  [Figs. 4(a) and 4(b)] indicates the presence of such polarization. As shown in the figure, the appearance of one more relaxation region in the doped film in the range of low frequencies takes place. If it is



MW polarization, the formation of the space charge mentioned above will be the consequence of this polarization. Since the last one gives the appearance of the  $E_{sc}$  field, it is convenient to watch its relaxation by presenting data of Fig. 9 in the form of complex electrical modulus  $M^*$  components<sup>21,22</sup> as follows:

$$M^*(\omega) = \frac{1}{\varepsilon^*(\omega)} = M' + iM'' = \frac{\varepsilon'}{\varepsilon'/2 + \varepsilon''/2} + i \frac{\varepsilon''}{\varepsilon'/2 + \varepsilon''/2}. \quad (6)$$

Frequency dependencies of the imaginary item  $M''$  for control and doped films are presented in Fig. 9(a). It can be seen that in the latter, the curve maximum is shifted by three

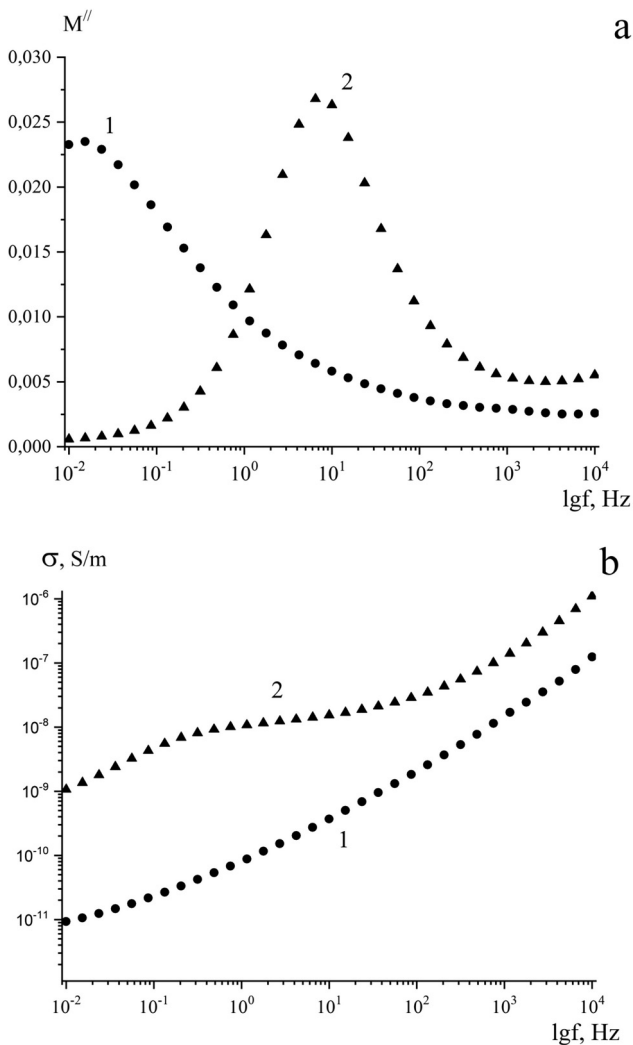


FIG. 9. Frequency dependencies of imaginary components of electrical modulus (a) and real component ac conductivity for original (1) and doped (2) films.

orders of magnitude to the side of high frequencies as compared with that of the control (non-doped) film. Clear registration of this relaxation process for the initial film is observed at higher temperatures.<sup>23</sup> The same patterns are registered for such relaxations of the space charge in the VDF-TrFE copolymer too.<sup>24</sup> Apparently, the higher conductivity of the doped film is the cause of such a substantial difference in relaxation times of the space charge formation in our case. Indeed, relaxation time of this process is presented as follows:

$$\tau_{MW} = \frac{\varepsilon_a \varepsilon_0}{A\sigma}. \quad (7)$$

As it can be seen from Fig. 9(b), low-frequency conductivity  $\sigma$  of the doped film turns out to be 2–3 orders of magnitude higher than that of the controlled one. According to equilibrium (7), it must result in a decrease of  $\tau_{MW}$  value and to a shifting of the dispersion region to the side of higher frequencies. Only that is seen in the experiment [Fig. 9(a)]. In light of such conclusions from low-voltage measuring, we must attribute current switches in the high fields to switching of the space charge field when high voltage pulse sign changes (Fig. 7).

Since the concentration of carriers in the doped film is significantly higher, we should expect a decrease in remnant polarization due to the capture of the marked carriers by the polar planes. This corresponds to partial internal compensation of the depolarization field. Such a process can lead to a decrease in local spontaneous (remnant) polarization and, accordingly, to a decrease in the initial signal local piezoresponse after local polarization. Data presented in Fig. 2(d) confirm this hypothesis, as in the undoped film the initial signal is more than 2 times higher.

The model of trapped carriers created by the dissociation of R6G by the polar planes of crystals is also confirmed by independent experiments on the study of phase transition of a ferroelectric-paraelectric in the copolymer P (VDF-TrFE) doped with the same dye. It has been found that in the paraelectric phase, where there are no polar phases and deep traps, respectively, an “abnormal” change in the characteristics of luminescence is shown.<sup>7</sup>

As it is mentioned above, the formation of space charge in the electric field also affects the kinetics of the decay of the piezoresponse signal after local polarization [Fig. 2(d)]. As can be seen, doping of the film leads to a strong change in the time dependence of the decay of the initial piezoelectric response. To quantify the decay of the piezoresponse signal, a Kohlrausch-Williams-Watts (KWW)<sup>25</sup> function was used

$$y = y_0 + \exp \left[ - \left( \frac{t}{\tau} \right)^\beta \right], \quad (8)$$

where  $\tau$  is the relaxation time and  $\beta$  is a parameter characterizing the distribution of relaxation times. Doping of the film leads to a change in  $\beta$  and a decrease in relaxation time by several times.

As shown above, there is a qualitative correlation between changes in macroscopic relaxation times of the formation of a space charge obtained in low electric fields [Fig. 9(a)].

## CONCLUSION

The analysis of spectral data and those of piezoforce microscopy shows that in the crystallization of the copolymer doped with R6G dye from solution, the dye tends to transit from the monomer form to the dimer one. Using the methods of optical microscopy and spectroscopy of piezo-force response, it has been found that in the film formed, microcrystals of micron size may appear. It was assumed that the dye aggregated forms can additionally structure the copolymer. The confirmation of such structuring was obtained by IR spectroscopy when the appearance of “anomalies” in the region of manifestation of methylene group valent vibrations was noticed. It is supposed that the structuring mentioned above proceeds due to the formation of labile hydrogen bonds of N-H...F-C type.

## ACKNOWLEDGMENTS

The work was supported by the Russian Federation for Basic Research (RFBR) (Grant No. N 18-03-00493). PFM and KPFM studies were performed at the Center for Shared Use “Material Science and Metallurgy” at the National University of Science and Technology “MISIS” and were supported by the Ministry of Science and Higher Education of the Russian Federation (Project No. 11.9706.2017/7.8).

## REFERENCES

- <sup>1</sup>The Application of Ferroelectric Polymers, edited by T. T. Wang, J. M. Herbert, and A. M. Glass (Blackie, Glasgow, 1988).
- <sup>2</sup>Ferroelectric Polymers—Chemistry, Physics and Applications, edited by H. S. Nalva (Marcel Dekker Inc., New York, 1995).
- <sup>3</sup>V. V. Kochervinskii, “The properties and applications of fluorine-containing polymer films with piezo- and pyro-activity,” *Russ. Chem. Rev.* **63**(4), 367 (1994).
- <sup>4</sup>See [www.piezotech.fr](http://www.piezotech.fr) for PVDF Shock Gauges.
- <sup>5</sup>V. V. Kochervinskii, “New electrostriction materials based on organic polymers: A review,” *Crystallogr. Rep.* **54**(7), 1146–1171 (2009).
- <sup>6</sup>L. Zhu and Q. Wang, “Novel ferroelectric polymers for high energy density and low loss dielectrics,” *Macromolecules* **45**, 2937–2954 (2012).
- <sup>7</sup>K. A. Verkhovskaya, V. M. Fridkin, A. V. Bune et al., *J. Appl. Phys.* **75**(1), 663 (1994).
- <sup>8</sup>R. Zhou, W. Liu, J. Kong, D. Zhou, G. Ding, Y. W. Leong, P. K. Pallathadka, and X. Lu, “Chemically cross-linked ultrathin electrospun poly(vinylidene fluoride-co-hexafluoropropylene) nanofibrous mats as ionic liquid host in electrochromic devices,” *Polymer* **55**, 1520–1526 (2014).
- <sup>9</sup>V. V. Kochervinskii, D. A. Kiselev, M. D. Malinkovich, A. S. Pavlov, N. V. Kozlova, and N. A. Shmakova, “Effect of the structure of a ferroelectric vinylidene fluoride-tetrafluoroethylene copolymer on the characteristics of a local piezoelectric response,” *Polym. Sci. A* **56**(1), 48 (2014).
- <sup>10</sup>V. V. Kochervinskii, D. A. Kiselev, M. D. Malinkovich, A. S. Pavlov, and I. A. Malyshkina, “Local piezoelectric response, structural and dynamic properties of ferroelectric copolymers of vinylidene fluoride-tetrafluoroethylene,” *Colloid Polym. Sci.* **293**, 533–543 (2015).
- <sup>11</sup>V. V. Kochervinskii, N. V. Kozlova, N. A. Shmakova, A. V. Kalabukhova, D. A. Kiselev, M. D. Malinkovich, M. A. Gradova, O. V. Gradov, and S. A. Bedin, “Influence of dye molecules on the polarization of ferroelectric vinylidene fluoride copolymer,” *Crystallogr. Rep.* **63**(6), 983–988 (2018).
- <sup>12</sup>V. V. Kochervinskii, “Ferroelectricity of polymers based on vinylidene-fluoride,” *Russ. Chem. Rev.* **68**(10), 821–857 (1999).
- <sup>13</sup>V. V. Kochervinskii, V. A. Glukhov, V. G. Sokolov, V. F. Romadin, E. M. Murasheva, Y. K. Ovchinnikov, N. A. Trofimov, and B. V. Lokshin, “Microstructure and crystallization isotropic films of the copolymer vinylidene fluoride and tetrafluoroethylene,” *Polym. Sci. A* **30**(9), 2100–2108 (1988).
- <sup>14</sup>D. V. Ageev, S. V. Patsaeva, B. D. Ryzhikov, V. N. Sorokin, and V. I. Yuzhakov, “Influence of temperature and ethanol content on aggregation of rhodamine 6G molecules in aqueous ethanol solutions,” *J. Appl. Spectrosc.* **75**(5), 653–657 (2008).
- <sup>15</sup>V. V. Kochervinskii, “Structure and properties of bulk polyvinylidene-fluoride and systems based on it,” *Russ. Chem. Rev.* **65**(10), 865–913 (1996).
- <sup>16</sup>V. V. Kochervinskii, L. O. Shoranova, S. A. Bondarenko, and A. E. Afonkin, “Applications of ferroelectric polymers as membranes, proton conductive materials and in gel polymer electrolytes,” *Int. J. Pharm. Technol.* **8**(4), 27238–27265 (2016).
- <sup>17</sup>J. Wang, Q. Fu, and Q. Zhang, “Inducing of dominant polar forms in poly(vinylidene fluoride) with super toughness by adding alkyl ammonium salt,” *Polymer* **53**, 5455–5458 (2012).
- <sup>18</sup>F. Wang, A. Lack, Z. Xie, P. Frübing, A. Taubert, and R. Gerhard, “Ionic-liquid-induced ferroelectric polarization in poly(vinylidene fluoride) thin films,” *Appl. Phys. Lett.* **100**, 062903 (2012).
- <sup>19</sup>V. V. Kochervinskii, D. A. Kiselev, M. D. Malinkovich, A. A. Korlyukov, B. V. Lokshin, V. V. Volkov, G. A. Kirakosyan, and A. S. Pavlov, “Surface topography and crystal and domain structures of films of ferroelectric copolymer of vinylidene difluoride and trifluoroethylene,” *Crystallogr. Rep.* **62**(2), 324–335 (2017).
- <sup>20</sup>J. Frenkel, “On pre-breakdown phenomena in insulators and electronic semi-conductors,” *Phys. Rev.* **54**, 647 (1938).
- <sup>21</sup>P. B. Macedo, C. T. Moynihan, and R. Bose, “The long time aspects of this correlation function, which are obtainable by bridge techniques at temperatures approaching the glass transition,” *Phys. Chem. Glass.* **13**, 171–179 (1972).
- <sup>22</sup>R. Richert, “The modulus of dielectric and conductive materials and its modification by high electric fields,” *J. Non-Cryst. Sol.* **305**, 29–39 (2002).
- <sup>23</sup>V. Kochervinskii, N. Kozlova, I. Malyshkina, and V. Astakhov, “Structural aspects of the high-temperature space charge relaxation in ferroelectric VDF/TFE 94/6 copolymer,” *Ferroelectrics* **531**, 1–21 (2018).
- <sup>24</sup>V. Kochervinskii, I. Malyshkina, S. Bedin, A. Korlyukov, M. Buzin, and R. Shakirzyanov, “Curie point and a space charge relaxation in ferroelectric poly(vinylidene fluoride-trifluoroethylene) copolymers with different thermal history,” *J. Appl. Polym. Sci.* **135**, 46186 (2018).
- <sup>25</sup>A. K. Jonscher, *Universal Relaxation Law: A Sequel to Dielectric Relaxation in Solids* (Chelsea Dielectrics Press, 1996).